

Chapter 7

The magnetoelastic coupling in $\text{Gd}_5(\text{Si}_x\text{Ge}_{1-x})_4$

7.1 Introduction

In this chapter, we study the effect of the magnetic field on the magnetostructural transition in $\text{Gd}_5(\text{Si}_x\text{Ge}_{1-x})_4$ alloys with $x \leq 0.5$. In particular, the variation of the transition field, H_t , with the transition temperature, T_t , is discussed as a function of x . This parameter, dH_t/dT_t , plays a key role in the scaling of ΔS , showing a different behaviour between the two compositional ranges ($x \leq 0.2$ and $0.24 \leq x \leq 0.5$) where the magnetostructural transition occurs. Moreover, dH_t/dT_t is related to the strength of the magnetoelastic coupling: in these compounds, the value of ΔS measured when the transition is field-induced coincides with the value measured when it is induced by the application of pressure [1]. Therefore, through the Clausius-Clapeyron equation (Eq. 1.17), it is shown that (see section 6.3)

$$\frac{\Delta M}{\Delta V} = \frac{dT_t}{dH_t} \frac{dP_t}{dT_t} . \quad (7.1)$$

Accordingly, a strong magnetoelastic coupling yields a small value of dH_t/dT_t .

7.2 $H - T$ diagram from magnetisation and DSC measurements

The systematic measurements of $\text{Gd}_5(\text{Si}_x\text{Ge}_{1-x})_4$ samples ($x=0, 0.05, 0.1, 0.18, 0.2, 0.25, 0.3, 0.365$ and 0.45) are detailed in section 5.2 (magnetisation) and 5.3 (DSC under field).

From both sets of measurements -DSC and $M(H)$ - the dependence of the transition temperature, T_t , on the transition field, H_t , can be evaluated independently.

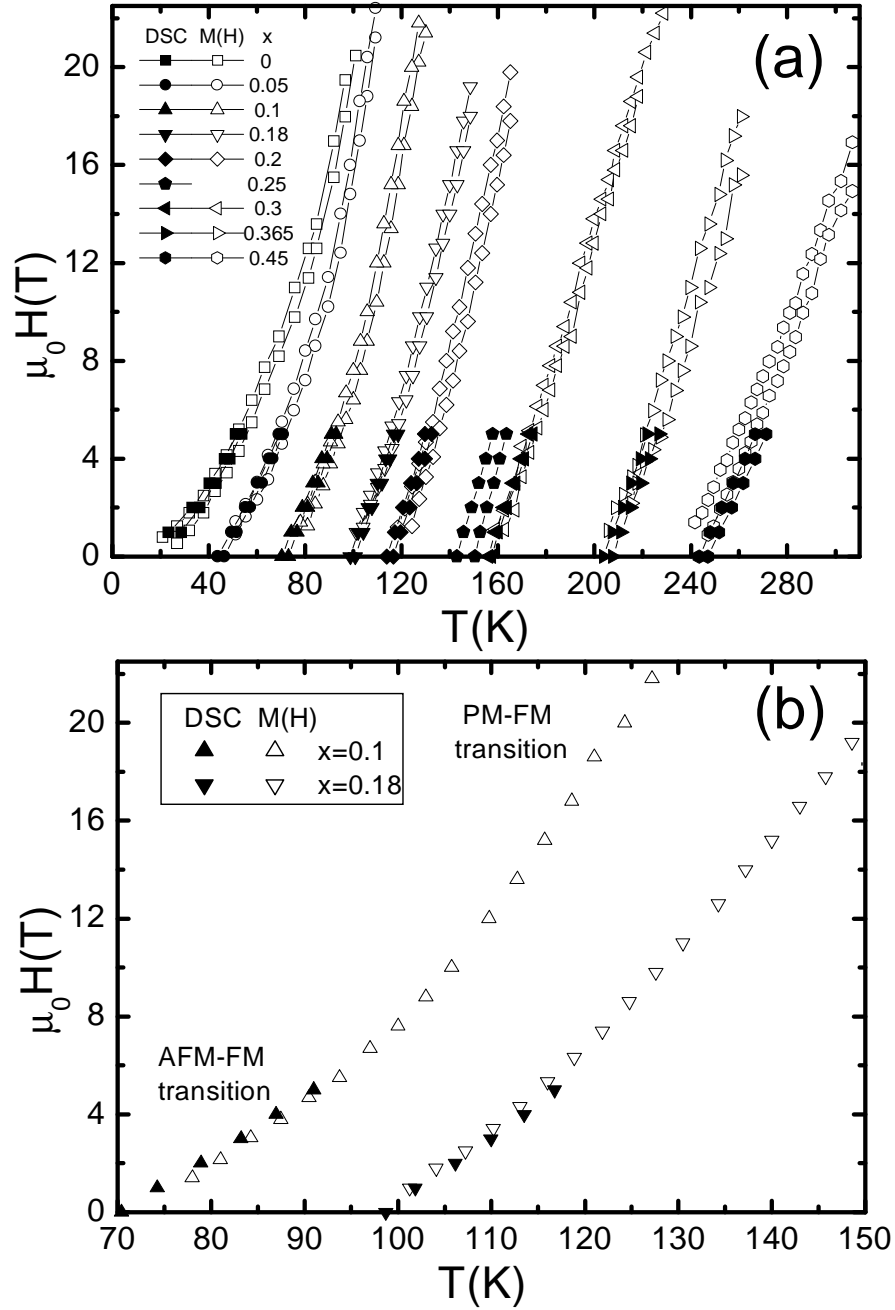


Figure 7.1: (a) Transition field, H_t , as a function of the transition temperature, T_t , for $Gd_5(Si_xGe_{1-x})_4$ (from $x=0$ to $x=0.45$) obtained from magnetisation isotherms (increasing and decreasing H) and DSC isofield data (cooling and heating). (b) Detail of panel (a) showing $H_t(T_t)$ for $x=0.1$ and $x=0.18$, on increasing H and cooling.

From magnetisation isotherms, $H_t(T)$ is defined at each temperature as the field corresponding to the inflection point within the transition region. Due to the hysteresis between increasing and decreasing field, two different values of H_t are obtained. From DSC, $T_t(H)$ is estimated at each applied field as the peak position in the dQ/dT curves. Due to the thermal hysteresis, two different values of T_t are obtained (see Table 6.1). Figure 7.1 (a) displays the transition field as a function of the transition temperature obtained from both DSC and $M(H)$ curves. Notice the good agreement between isofield and isothermal data. T_t values at zero field obtained by $M(H)$ (extrapolated) and DSC are displayed in Table 7.1 for all compositions, being in agreement with the phase diagram (Fig. 2.2). Interestingly, for $0.24 \leq x \leq 0.5$, where only the PM-to-FM transition occurs, $H_t(T_t)$ shows a linear behaviour over the whole field range, while for $x \leq 0.2$, the slope of $H_t(T_t)$ varies progressively from a low-field value (AFM-FM transition) to a high-field value (PM-FM transition). This effect is illustrated in Fig. 7.1 (b), which shows a detail of Fig. 7.1 (a) for $x=0.1$ and $x=0.18$ curves. Such a progressive change in the slope is due to the fact that, at high fields, the magnetostructural transition overlaps the second order PM-AFM transition (Fig. 5.5 (c)), giving rise to a unique PM-FM transition.

7.3 dH_t/dT_t and magnetoelastic coupling

Figure 7.2 compiles, for all compositions, the values of the slope, dH_t/dT_t , as a function of x , determined from the data in Fig. 7.1. For $x \leq 0.2$, two limiting values of dH_t/dT_t corresponding to the low and high field regimes are displayed, while a single value of dH_t/dT_t is found for $0.24 \leq x \leq 0.5$. Datum for $x=0.5$ is taken from Ref. [2]. We note the linear dependence of dH_t/dT_t on x , which is decreasing for the PM-FM transition (solid line in Fig. 7.2), while it is increasing for the AFM-FM transition (dashed line in Fig. 7.2). Both lines meet at the composition range where the second-order transition disappears ($0.2 < x < 0.24$), in agreement with the phase diagram (Fig. 2.2 and Ref. [3]). The value of dH_t/dT_t for $x=0$ at high fields is lower than expected because a field higher than 23 T (the maximum available in the present work) must be applied to fully induce the PM-FM transition. Values of dH_t/dT_t obtained from DSC and $M(H)$ measurements for all compositions are displayed in Table 7.2 and compared with values given in literature.

The strength of the magnetoelastic coupling is associated with the field dependence of T_t (*i.e.*, a strong magnetoelastic coupling yields a small value of dH_t/dT_t) as demonstrated in the introduction of this chapter. Consequently, the decrease in dH_t/dT_t with increasing x for the PM-FM transition indicates a strengthening of the magnetoelastic coupling. This may be explained by considering that FM

x	ID	Heat T.	$T_i(H = 0)$ (K)			
			DSC		$M(H)$	
			cool.	heat.	incr. H	decr. H
0	#1	NO	~13*	~20*	~15*	~22*
0.05	#1	T4+Q	43.8	46.5	44.5	45.9
0.1	#1	NO	70.4	73.1	73.2	76.5
0.18	#1	NO	-	-	103.7	106.1
		T4	98.7	100.9	97.8	99.5
0.2	#1	NO	113.9	116.6	114.6	120.5
0.25	#2	NO	143.0	150.5	-	-
0.3	#2	NO	169.7	177.5	-	-
		T4+Q	156.1	157.3	156.6	160.4
0.365	#3	NO	200.7	204.5	204.3	209.3
0.45	#7	NO	247.2	252.3	245.1	252.2
		T4	243.5	247.1	238.0	244.9

Table 7.1: Transition temperature at zero field, $T_i(H = 0)$, at the first-order transition obtained by extrapolating $T_i(H)$ obtained from $M(H)$, and also by DSC at $H=0$ for all measured samples. *These values are valid after the low-temperature FM phase has been induced irreversibly in the $x=0$ compound by the application of a high enough magnetic field (see section 2.4.1).

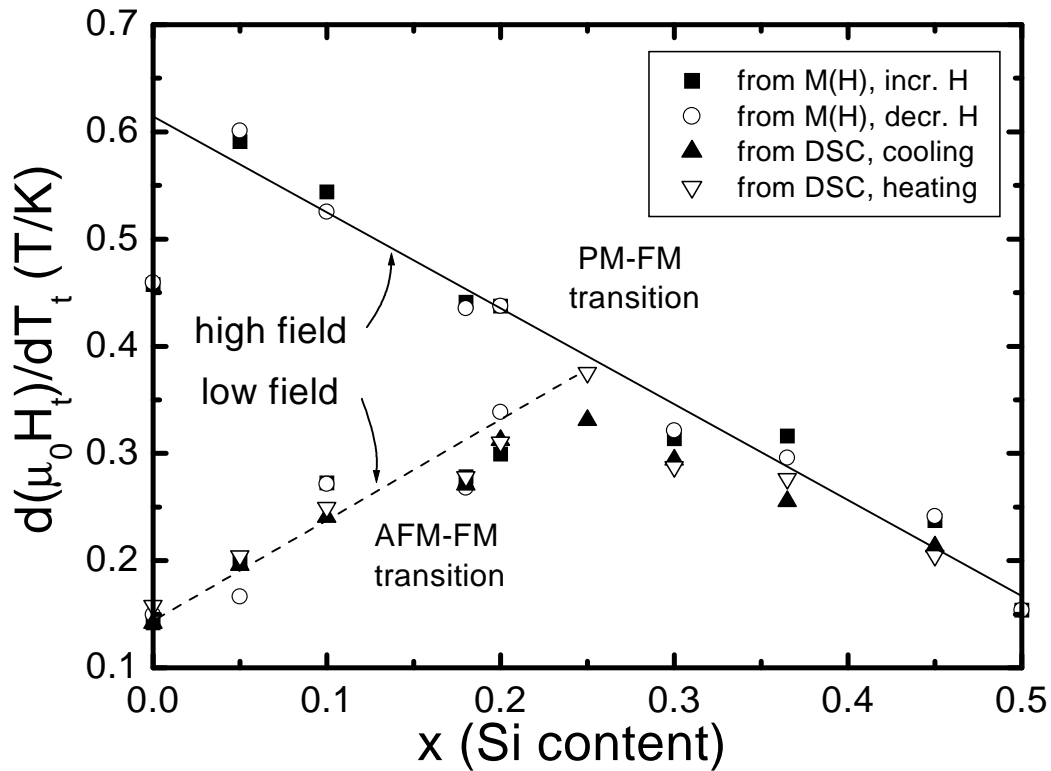


Figure 7.2: Slope of $H_i(T_i)$ calculated from data in Fig. 7.1. For $x=0.25, 0.3, 0.365, 0.45$ and 0.5 (the latter from Ref. [2]) a single slope is obtained, which corresponds to the PM-FM transition. For $x=0, 0.05, 0.1, 0.18$ and 0.2 two limiting slopes are obtained: a low-field value (associated with the AFM-FM transition) and a high-field value (associated with the PM-FM transition). Solid and dotted lines are a guide to the eye.

x	$d(\mu_0 H_i)/dT_i$ (T/K)						Literature
	DSC		$M(\text{low } H)$		$M(\text{high } H)$		
	cool.	heat.	inc. H	dec. H	inc. H	dec. H	
0	0.142	0.158	0.142	0.149	0.458	0.460	0.125 [4]
0.05	0.196	0.204	0.202	0.166	0.591	0.601	
0.08							0.294 [5]
0.1	0.241	0.250	0.273	0.271	0.544	0.525	0.27 [3], 0.26 [3]
0.18	0.271	0.278	0.278	0.268	0.441	0.435	
0.2	0.312	0.311	0.299	0.338	0.437	0.437	
			$M(H)$				
			inc. H	dec. H			
0.25	0.331	0.376	-	-			
0.3	0.294	0.287	0.314		0.321		
0.365	0.255	0.277	0.316		0.296		
0.375							0.28 [6, 7], 0.25 [8],
0.43							0.23 [9]
0.45	0.213	0.205	0.237		0.241		0.21 [1], 0.22 [10]
0.5							0.154 [2], 0.18 [11], 0.14 [12]

Table 7.2: dH_i/dT_i obtained from $M(H)$ and DSC under magnetic field for all measured samples. For $x \leq 0.2$, two limiting values are obtained from magnetisation data. Values from different references are also compiled for comparison.

exchange interactions are stronger for increasing x , as suggested by the magnetic phase diagram, where T_i increases linearly with x (Fig. 2.2). The fact that dH_i/dT_i for the PM-FM transition has continuous behaviour, although the PM phase is monoclinic for $0.24 \leq x \leq 0.5$ and orthorhombic-II for $x \leq 0.2$, suggests that the magnetoelastic coupling is weakly dependent on the actual crystallographic structure. Concerning the AFM-FM transition, and taking into account that the structural transition is the same (for $x \leq 0.2$) or very similar (for $0.24 \leq x \leq 0.5$) to that occurring in the PM-FM case, the increase in dH_i/dT_i with x may be related to the fact that the transition involves two ordered magnetic phases (FM and AFM). Fig. 7.2 thus summarizes the behavior of the first-order transition in $\text{Gd}_5(\text{Si}_x\text{Ge}_{1-x})_4$ as a function of x , T and H .

The behaviour of dH_i/dT_i with x is relevant in the scaling of $|\Delta S|$ which appears in $\text{Gd}_5(\text{Si}_x\text{Ge}_{1-x})_4$ alloys (Chapter 6): taking into account the Clausius-Clapeyron equation and as ΔM always decreases with T , $|\Delta S|$ thus increases with T_i for $x \leq 0.2$ when the AFM-FM transition takes place, due to the larger increase of dH_i/dT_i with T_i as compared to the decrease in ΔM with T_i . In contrast, $|\Delta S|$ decreases with T_i for the PM-FM transition, since the increase in dH_i/dT_i with T_i is not large enough as to overcome the decrease in ΔM . Therefore, although the main feature of the scaling of $|\Delta S|$ with T_i is not only determined by dH_i/dT_i vs T_i , the particular dependence of dH_i/dT_i on x and H enables the scaling.

7.4 Conclusions

The variation of the transition field with the transition temperature, dH_i/dT_i , has been studied in $\text{Gd}_5(\text{Si}_x\text{Ge}_{1-x})_4$ for all the range of compositions where the first-order transition occurs, $0 \leq x \leq 0.5$. Taking into account the behaviour of dH_i/dT_i as a function of x and that ΔM decreases monotonously with T_i , it is shown that dH_i/dT_i governs the scaling of ΔS with T_i reported in Chapter 6, giving further evidence that the origin of this scaling is the magnetoelastic nature of the transition. Moreover, two distinct behaviors for dH_i/dT_i have been found on the two compositional ranges where the magnetostructural transition occurs, thus showing the difference in the strength of the magnetoelastic coupling of this system.

Bibliography

- [1] L. Morellon, P. A. Algarabel, M. R. Ibarra, J. Blasco, B. García-Landa, Z. Arnold, and F. Albertini, *Phys. Rev. B* **58**, R14721 (1998).
- [2] A. Giguère, M. Földeàki, B. Ravi Gopal, R. Chahine, T. K. Bose, A. Frydman, and J. A. Barclay, *Phys. Rev. Lett.* **83**, 2262 (1999).
- [3] L. Morellon, J. Blasco, P. A. Algarabel, and M. R. Ibarra, *Phys. Rev. B* **62**, 1022 (2000).
- [4] E. M. Levin, K. A. Gschneidner, Jr., and V. K. Pecharsky, *Phys. Rev. B* **65**, 214427 (2002).
- [5] V. K. Pecharsky and K. A. Gschneidner, Jr., *Adv. Cryog. Eng.* **43**, 1729 (1998).
- [6] E. M. Levin, V. K. Pecharsky, and K. A. Gschneidner, Jr., *Phys. Rev. B* **62**, R14625 (2000).
- [7] E. M. Levin, V. K. Pecharsky, and K. A. Gschneidner, Jr., *J. Magn. Magn. Mater.* **231**, 135 (2001).
- [8] E. M. Levin, V. K. Pecharsky, K. A. Gschneidner, Jr., and P. Tomlinson, *J. Magn. Magn. Mater.* **210**, 181 (2000).
- [9] V. K. Pecharsky and K. A. Gschneidner, Jr., *Appl. Phys. Lett.* **70**, 3299 (1997).
- [10] L. Morellon, J. Stankiewicz, B. García-Landa, P. A. Algarabel, and M. R. Ibarra, *Appl. Phys. Lett.* **73**, 3462 (1998).
- [11] V. K. Pecharsky and K. A. Gschneidner, Jr., *Phys. Rev. Lett.* **78**, 4494 (1997).
- [12] E. M. Levin, V. K. Pecharsky, and K. A. Gschneidner, Jr., *Phys. Rev. B* **60**, 7993 (1999).